Journal of Medicinal Chemistry

Article

Probing Molecular Interactions between human Carbonic Anhydrases (hCAs) and a Novel Class of Benzenesulfonamides

Elvira Bruno, Maria Rosa Buemi, Anna Di Fiore, Laura De Luca, Stefania Ferro, Andrea Angeli, Roberto Cirilli, Daniele Sadutto, Vincenzo Alterio, Simona Maria Monti, Claudiu T Supuran, Giuseppina De Simone, and Rosaria Gitto

J. Med. Chem., **Just Accepted Manuscript** • Publication Date (Web): 28 Apr 2017

Probing Molecular Interactions between human Carbonic Anhydrases (hCAs) and a Novel Class of Benzenesulfonamides

*Elvira Bruno,[a] Maria Rosa Buemi,[a] Anna Di Fiore,[b] Laura De Luca,[a] Stefania Ferro,[a] Andrea Angeli,[c] Roberto Cirilli,[d] Daniele Sadutto,[d] Vincenzo Alterio,[b] Simona Maria Monti,[b] Claudiu T. Supuran,[c] Giuseppina De Simone,[b] Rosaria Gitto[a]**

[a]Dipartimento di Scienze Chimiche, Biologiche, Farmaceutiche ed Ambientali (CHIBIOFARAM), Università degli Studi di Messina, Viale Annunziata, I-98168, Messina.

[b]Istituto di Biostrutture e Bioimmagini-CNR, Via Mezzocannone 16, 80134, Napoli

[c]Dipartimento NEUROFARBA, Università di Firenze, Via Ugo Schiff 6, I-50019 - Sesto Fiorentino.

[d]Centro nazionale per il controllo e la valutazione dei farmaci, Istituto Superiore di Sanità, V.le Regina Elena, 299, 00161 Roma.

Keywords: human Carbonic Anhydrases; isoquinoline-sulfonamides; HPLC; X-ray crystallography; docking studies

Abstract: On the basis of X-ray crystallographic studies of the complex of hCA II with 4-(3,4-dihydro-1*H*-isoquinoline-2-carbonyl)benzenesulfonamide (**3**) (PDB code 4Z1J), a novel series of 4-(1-aryl-3,4-dihydro-1*H*-isoquinolin-2-carbonyl)benzenesulfonamides (**23-33**) was designed. Specifically, our idea was to improve the selectivity toward druggable isoforms through the introduction of additional hydrophobic/hydrophilic functionalities. Among the synthesized and tested compounds, the (*R,S*)-4-(6,7-dihydroxy-1-phenyl-3,4-tetrahydroisoquinoline-1*H*-2-carbonyl)benzenesulfonamide (**30**) exhibited a remarkable inhibition for the brain-expressed hCA VII (K_i = 0.20 nM) and selectivity over wider distributed hCA I and hCA II isoforms. By enantioselective HPLC we solved the racemic mixture and ascertained that the two enantiomers (**30a** and **30b**) are equiactive inhibitors for hCA VII. Crystallographic and docking studies revealed the main interactions of these inhibitors into the carbonic anhydrase (CA) catalytic site, thus highlighting the relevant role of non-polar contacts for this class of hCA inhibitors.

Introduction

Human carbonic anhydrases (hCAs, EC 4.2.1.1) are metalloenzymes that catalyse the reversible hydration of carbon dioxide to bicarbonate and proton. The hCA family comprises 15 different α-CA isoforms, of which five are cytosolic (CA I-III, CA VII and CA XIII), four are membrane-bound (CA IV, CA IX, CA XII, and CA XIV), two are mitochondrial (CA VA and CA VB), and one is secreted into saliva (CA VI). hCAs are involved in various physiological processes (gluconeogenesis, lipogenesis, and ureagenesis). However, their abnormal levels or activities have been often associated with several diseases such as cancer, epilepsy, obesity, glaucoma, etc.[1-6] For this reason, CA isoforms have become relevant targets for the design of inhibitors with biomedical applications.[5, 7, 8]

hCA VII, hCA IX, hCA XII and hCA XIV are among the most interesting hCA isoforms. hCA VII is mainly expressed in the cortex, hippocampus and thalamus regions within the mammalian brain where it is involved in generating neuronal excitation and seizures[4, 9] as well as in neuropathic pain control.[10] hCA IX is overexpressed in many solid tumours associated with the hypoxic phenotype, where it is involved in critical processes connected with cancer progression.[11,12-22] Recently, it was demonstrated that also hCA XII is a tumor-associated isoform, thus emerging as innovative target for the development of anticancer agents.[22] Finally, hCA XIV is a transmembrane isozyme with an extracellularly oriented active site; it is highly abundant in neurons and axons in the murine and human brain, where it seems to play an important role in modulating excitatory synaptic transmission.[23, 24]

Although, the first generation of CA inhibitors (CAIs), such as acetazolamide (**AAZ, 1**) and topiramate (**TPM**, **2**) (Chart 1), were able to strongly bind hCA VII, hCA IX, hCA XII and hCA XIV, they were also strong inhibitors of the ubiquitous hCA I and hCA II isoforms, displaying many undesired side-effects. Consequently, many research efforts have been recently dedicated to the design of new CAIs able to target selectively hCA VII, hCA IX, hCAXII and hCA XIV.[25]

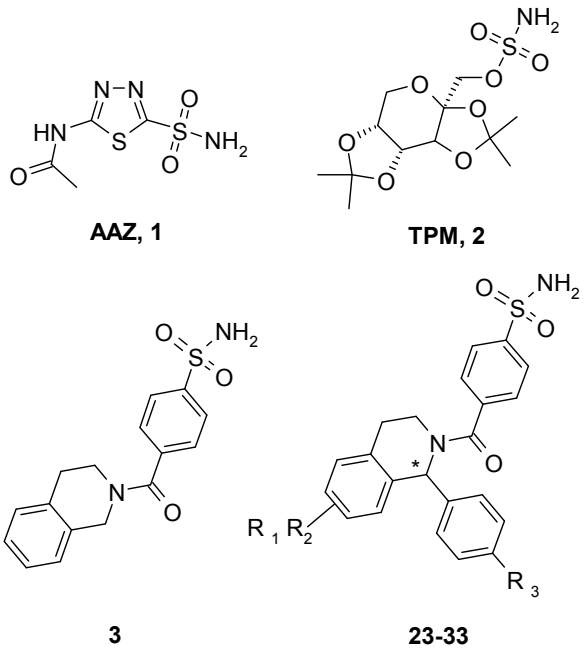

Chart 1. Chemical structures of selected hCAIs (**1-3**) and designed compounds (**23-33**)

Among the CAIs so far developed, sulfonamide based compounds are the most studied. These compounds bind the catalytic zinc ion through the deprotonated nitrogen of the sulfonamide moiety, blocking the CA enzymatic activity.[26-40] The hCA isoform selectivity of sulfonamide-based CAIs is tuned by the remaining molecular fragment, which can interact with hydrophobic/hydrophilic residues delimiting the CA-catalytic site.[38, 41-47] So the high selectivity towards several isoforms is controlled by profitable interactions between the hydrophobic/hydrophilic residues on the CA cleft and suitable functional groups of the most selective hCAIs.[24, 48, 49]

We have recently reported a new series of heteroaryl-N-carbonylbenzenesulfonamides as CAIs.[50] Among them, the 4-(3,4-dihydro-1*H*-isoquinoline-2-carbonyl)benzenesulfonamide (**3**, Chart 1) had significant inhibitory effects against hCA VII, hCA IX, and hCA XIV. Herein we report the synthesis, structural characterization and evaluation of inhibitory effects of eleven (*R,S*)-4-(1-aryl-3,4-dihydro-1*H*-isoquinoline-2-carbonyl)benzenesulfonamides (**23-33**, Chart 1) inspired by the prototype **3**. In particular, we investigated the introduction of an alkoxy or hydroxyl substituent on 6/7-positions of isoquinoline system combined with the presence of an aryl-substituent at the C-1

position. Specifically, the 6 and/or 7 substituents (R_1R_2) could furnish new H-bonding contacts; whereas the C-1 fragment could add a new hydrophobic anchoring moiety, that might be useful to strengthen the network of non-polar interactions with hydrophobic residues within catalytic site. To enhance the hydrophobic interactions we also examined the effects of an additional halo-substituent (R_3) at para position of C-1 phenyl ring. The introduction of C-1 phenyl ring generates a chiral center that could furnish a couple of enantiomers with different inhibitory effects. Thereby, we decided to perform the resolution of racemic mixtures of selected inhibitors to explore the impact of stereochemistry on CA inhibition. Moreover, experimental and computational analyses have been performed to highlight the interactions of these molecules within the active site. Specifically, we studied the crystallographic structures of the adducts of the most active compounds of the series with hCA II and performed docking simulations to identify the binding poses of these molecules within the hCA VII catalytic site. Finally, we have compared the solved crystal structures with docking poses to search for structural information about the isoform-selectivity profile.

Results and discussion

Synthesis. The designed (*R,S*)-4-(1-aryl-3,4-dihydro-1*H*-isoquinoline-2-carbonyl)benzenesulfonamides (**23-33**) were synthesized by the procedure described in Scheme 1. Following a previously reported method,[51] we prepared the 1-phenyl-1,2,3,4-tetrahydroisoquinolines **17-22** in Microwave Assisted Organic Synthesis conditions by a Pictet-Spengler approach from phenylethylamine derivatives **4-6** and suitable benzaldehyde derivatives **7-10**. Specifically, in the first step we obtained the imine intermediates **11-16**, which were treated with trifluoroacetic acid (TFA) to provide the desired isoquinolines **17-22** as racemic mixtures. Successively, amines **17-22** reacted with the 4-(aminosulfonyl)benzoic acid to give desired *N*-substituted isoquinolines **23-28**. The 6,7-dimethoxy and 6-methoxy derivatives **23, 25-28** were further transformed into the corresponding hydroxyl analogues **29-33** by treatment with BBr_3 in the

presence of anhydrous CH_2Cl_2 and under an atmosphere of N_2. The chemical characterization of intermediates and final compounds was supported ^{1}H-NMR (see Experimental section). The purity of tested compounds was confirmed by elemental analysis.

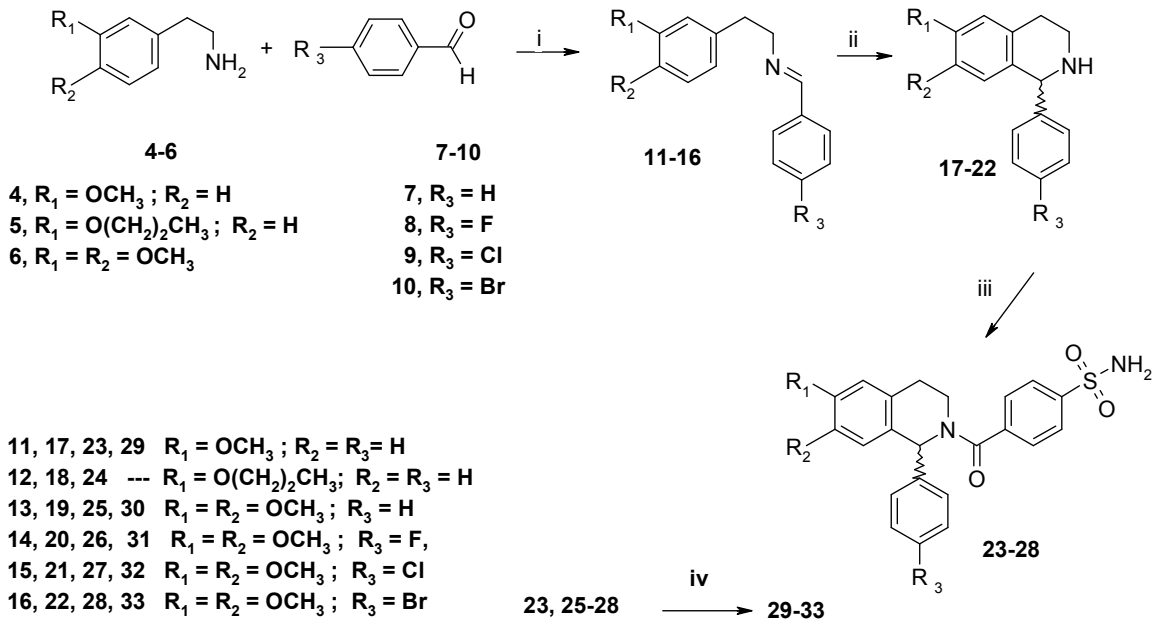

Scheme 1. Reagents and conditions: i) MW: 10 min, 90°C, 150 W; ii) TFA, MW: 10 min, 90 °C, 150 W; iii) 4-(aminosulfonyl)benzoic acid, HBTU, TEA, DCM, rt, overnight; iv) BBr_3(1 M in DCM), DCM, rt, overnight.

Carbonic Anhydrase Inhibition. The CA inhibitory effects of obtained 4-(1-aryl-3,4-dihydro-1*H*-isochinolin-2-carbonyl)benzenesulfonamides (**23-33**) were measured for human CA I, CA II, CAVII, CA IX, CA XII and CA XIV; results are summarized in Table 1 and compared with K_i values of prototype **3,** AAZ (**1**) and TPM (**2**) as reference compounds. For the preliminary investigation, we have tested the racemic mixtures of all new synthesized compounds.

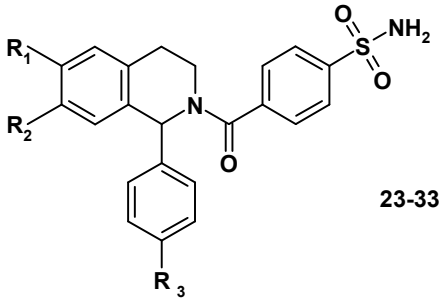

23-33

Table 1. K_i values of arylsulfonamide derivatives **3**, and **23-33** against hCA I, hCA II, hCA VII, hCA IX, hCA XII and hCA XIV. For comparison purpose, data of **AAZ** and **TPM** were also reported.

				K_i(nM)[a]					
	R_1	R_2	R_3	hCA I	hCA II	hCA VII	hCA IX	hCA XII	hCA XIV
3[b]	H	H	---	76.2	7.7	9.20	7.50	n.t.	9.6
23	OCH_3	H	H	39.1	5.3	1.40	39.2	18.7	3.2
24	OC_3H_7	H	H	850	33.2	84.4	44.5	6.7	25.6
25	OCH_3	OCH_3	H	16.4	6.9	7.30	4.90	60.3	4.3
26	OCH_3	OCH_3	F	6.9	0.84	0.53	9.10	4.3	374
27	OCH_3	OCH_3	Cl	10.9	5.5	0.77	91.4	933	325
28	OCH_3	OCH_3	Br	38.9	16.9	3.80	90.9	847	4010
29	OH	H	H	6.2	4.5	0.35	50.6	4.9	2.9
30	OH	OH	H	9.3	3.5	0.20	36.9	4.7	3.3
31	OH	OH	F	2.2	0.21	0.51	8.20	4.3	346
32	OH	OH	Cl	3.5	0.29	0.40	9.00	7.6	2915
33	OH	OH	Br	3.4	0.28	0.33	81.5	9.3	3930
TPM[b]				250	10	0.90	58	3.8	1460
AAZ[b]				250	12.1	2.50	25.	5.7	41

[a]Errors are in the range of ± 10 % of the reported value, from 3 different assays. [b]Data are taken from Reference 50.

n.t. = not tested

Firstly, we can observe that the introduction of a methoxy-group at C-6 position and a phenyl ring at C-1 was well tolerated except for hCA IX, so that compound **23** displayed similar inhibitory effects than those of prototype **3**. In turn, the replacement of the methoxy group with propoxy one (see compound **24**) generally resulted in reduction of inhibition against studied hCAs. The presence of an additional methoxy group at C-7 position (i.e. compound **25** vs **23**) resulted in about 3-fold drop in potency of inhibition against hCA XII isoform and a 5-fold improvement against hCA IX (see Table 1). Secondly, the introduction of a fluorine atom at para position of C-1 phenyl ring (compound **26**) resulted in a remarkable inhibition of hCA II and hCA VII isoforms for compound **26**; whereas this modification led to a loss of activity toward hCA XIV. Then, the replacement of the fluorine atom with chlorine or bromine atoms induced a remarkable reduction of potency for hCA XII and hCA XIV isoforms for compounds **27** and **28** compared with fluorine analogue **26**. It was possible to observe that the increasing size of the halogen atom was detrimental for inhibition of all studied isoforms. The degree of CA inhibitory potency was the following 4-F>4-Cl>4-Br.

Finally, we examined the impact on CA inhibition of the removal of methyl group of 6/7 methoxysubstituents on isoquinoline nucleus. The monohydroxy-derivative **29** and dihydroxy-derivative **30** displayed a very similar inhibitory potency against studied hCA isoforms. Specifically, they showed remarkable potency as hCA VII inhibitors (K_i values of 0.20 and 0.35 nM, respectively for compound **30** and **29**). Interestingly, the 4-halophenyl derivatives **31-33** proved to be very active inhibitors displaying K_i values ranging from 0.21 to 0.51 nM against hCA II and hCA VII. By analysing the hCA VII K_i values shown by hydroxyl compounds **29-33**, we found a flat influence of the steric and electronic effects of the para-phenyl substituent, thus suggesting that this substituent does not establish crucial contacts within catalytic site. Moreover, compounds **31-33** showed high inhibitory potency for hCA I, hCA IX and hCA XII. The replacement of chlorine atom of compound **32** (K_i value of 9.0 nM) with bromine atom gave about ten-fold reduction of potency (i.e. compound **33**, K_i value of 81.5 nM) exclusively for hCA IX inhibition. On the contrary, the presence of halogen atoms gave up to 1200-fold drop of potency

against hCA XIV (i.e. compound **33** *vs* compound **30**). These data might suggest that the increase in atomic radius impair the binding recognition within catalytic site of hCA XIV.

Results displayed in Table 1 can be summarized as follows. By combining the hydroxyl substituents on 6/7 positions of isoquinoline nucleus with the introduction of aryl substituent at C-1 position, a series of very active CA inhibitors was obtained. These structural modifications generally led to the enhancement of activity up to subnanomolar concentration especially toward hCA VII isoform when compared with prototype **3** and well-known reference compound **AAZ**. Interestingly, the presence of 4-halophenyl substituent at C-1 generally resulted in very low inhibition of hCA XIV isoform.

Enantiomeric resolution. Since all synthesized compounds contain a stereogenic centre and it is recognized that the molecular chirality adds an additional level of specificity and complexity in achieving of biological activity, the enantiomers of most promising derivatives (compounds **23**, **25**, **29** and **30**) were separated by enantioselective HPLC. The potential inhibitory activity against CAs was evaluated for eight compounds **23a**, **23b**, **25a**, **25b**, **29a**, **29b**, **30a**, and **30b**.

Specifically, the complete HPLC resolution was achieved on polysaccharide-based chiral stationary phases (CSPs) using normal-phase eluents. Typical chromatograms of the HPLC enantioseparation on an analytical scale are shown in Figure 1. The optimized analytical enantioselective conditions were successfully scaled up to a multi-milligram level using semi-preparative 250 mm x 10 mm I.D. columns. Both enantiomers of each compound were isolated with high enantiomeric purity (enantiomeric excess > 99 %).

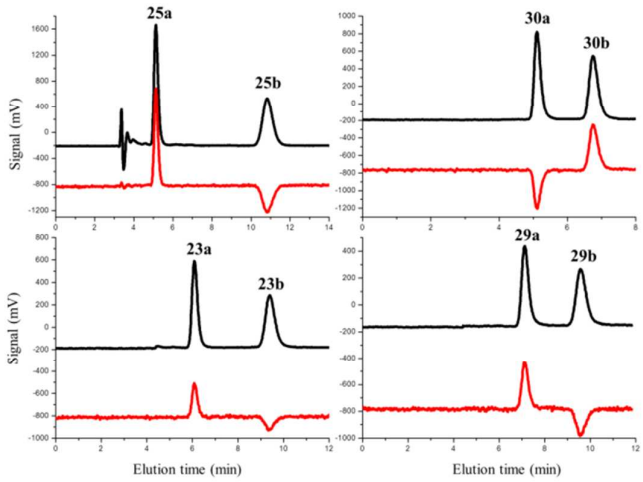

Figure 1. Analytical HPLC resolution of **23**, **25**, **29** and **30**. Column: Chiralpak AS-H 250 mm x 4.6 mm i.d. (**23**, **25**, **29**) and Chiralpak IA 250 mm x 4.6 mm i.d. (**30**); mobile phase: n-hexane/ethanol/TFA 20/100/0.1 (**23**, **25**, **29**) an n-hexane/ethanol/TFA 40/60/0.1 (**30**); flow rate: 1 mL/min; temperature: 25 (30) and 40 °C (23, 25, 29); detector: UV (black line) and CD (red line) at 280 nm. The letters a and b denote the enantiomer elution order.

The enantiomeric nature of the samples obtained on mg-scale was demonstrated by circular dichroism (CD) analysis (see Supporting Information). The assignment of absolute configuration of the enantiomerically pure **30a** and **30b** has been determined by X-ray studies (*vide infra*). For each single enantiomer CA inhibitory effects were screened. By analysing the K_i values summarized in Table 2 we can observe that there is not significant influence of the stereochemistry on the CA inhibitory effects. With the exception of **23b,** which proved to be slightly less potent than **23a**, both enantiomers were found to be equiactive inhibitors at low nanomolar concentrations. This evidence suggests that the two enantiomers could assume binding poses, which are effective for CA inhibition.

Table 2. K_i values against hCA I, hCA II, hCA VII, hCA IX, hCA XII and hCA XIV by each single enantiomer of selected arylsulfonamides **23**, **25, 29** and **30**

			K_i nM					
	R_1	R_2	hCA I	hCA II	hCA VII	hCA IX	hCA XII	hCA XIV
23a	OCH_3	H	15.6	4.8	0.77	25.3	13.0	2.4
23b	OCH_3	H	77.8	6.0	4.1	58.7	30.6	6.1
25a	OCH_3	OCH_3	16.6	4.9	9.2	5.0	19.7	4.3
25b	OCH_3	OCH_3	16.0	8.9	5.4	4.8	45.5	4.3
29a	OH	H	7.5	5.0	0.80	73.2	8.6	6.3
29b	OH	H	5.6	3.2	0.49	39.8	3.0	1.7
30a	OH	OH	9.3	3.3	0.21	32.7	5.8	3.2
30b	OH	OH	9.3	3.6	0.19	39.2	3.3	3.4

[a]Errors in the range of ± 10 % of the reported value, from 3 different assays.

X-ray Crystallography. To identify the key interactions involved into protein/inhibitor recognition of this CAI class, the crystal structure of the adduct which hCA II forms with one of its best inhibitors, namely compound **30**, was solved. hCA II was selected as model isoform for crystallization, since it easily forms crystals and many studies have been reported on its adducts with different classes of inhibitors.[40] In particular, the two **30** enantiomers, namely (*R*)-**30a** and (*S*)-**30b**, were singularly used for soaking experiments. Data collection and refinement of both adducts were performed as described in the experimental section (see Supporting Information for statistics).

In both complexes, inspection of the initial Fo − Fc electron density maps immediately revealed the binding of the inhibitor molecule in the active site. The inhibitor binding does not alter hCA II three-dimensional structure. Indeed, the r.m.s.d. values calculated by superposition of all the Cα atoms of the hCA II/**30a** and hCA II/**30b** adducts with those of the native protein were 0.26 Å and 0.25 Å, respectively.

Active site analysis of the two structures showed that the sulfonamide moiety of the two inhibitors maintains a binding mode to the protein similar to that observed for other CAIs containing the same group.[40] Indeed, the deprotonated nitrogen atom displaces the hydroxyl ion/water molecule present in the native enzyme and coordinates the zinc ion with a tetrahedral geometry, while additional hydrogen bond interactions with residue Thr199 further contribute to stabilize the binding (Figure 2A and 2B).

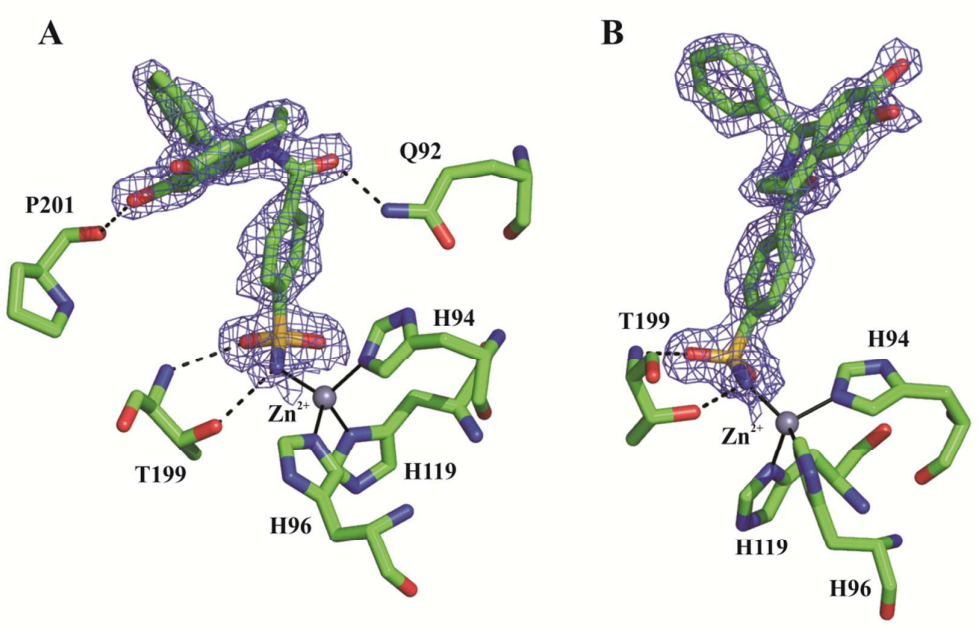

Figure 2. Active site region of the hCA II/(*R*)-**30a** (**A**), hCA II/(*S*)**30b** (**B**) adducts showing the σA-weighted |2Fo-Fc| OMIT map (contoured at 1.0 σ) relative to the inhibitor molecule. The zinc ion coordination and polar interactions are also reported.

The orientation of the organic scaffold of the two inhibitors is instead rather peculiar. Indeed, in both cases, the phenyl-substituent at the C-1 position is located in the hydrophobic region of the active site, in a small pocket delimited by residues Phe131, Val135, Leu198 and Pro202, whereas the isoquinoline ring is oriented toward a poorly explored area of the active site, located at the border between the hydrophobic and hydrophilic regions (Figure 3).[40]

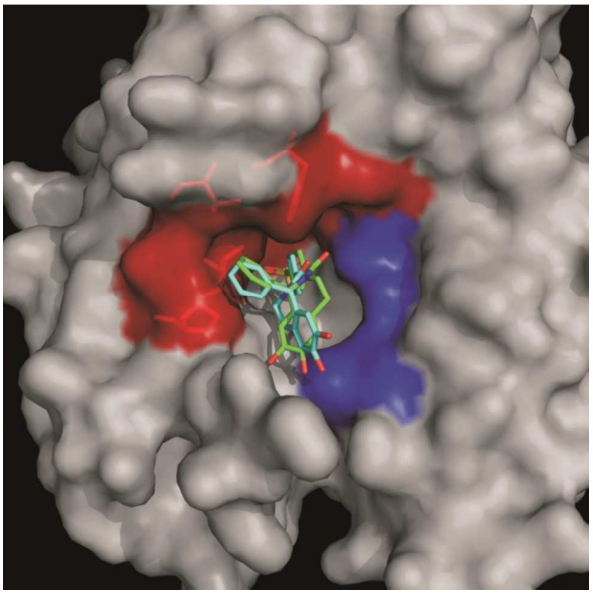

Figure 3. Solvent accessible surface of hCA II/inhibitor adducts. The hydrophobic region of the active site is shown in red, whereas the hydrophilic one in blue. Residues delimiting the small pocket interacting with the C-1 phenyl substituent of both inhibitors (Phe131, Val135, Leu198 and Pro202) are shown in stick representation.

By the superposition of the hCA II/**30a** and hCA II/**30b** structures, it is evident that small differences are present in the orientation of the organic scaffold of the two inhibitors, due to the diverse chirality of the C-1 atom (Figure 3). As a consequence (*R*)-**30a** establishes with the enzyme two hydrogen bonds, involving both the carbonyl oxygen and one of the two hydroxyl groups (Figure 2A), which instead are not present in the hCA/(*S*)-**30b** structure (Figure 2B). Nevertheless, the two inhibitors retain the same affinity for the enzyme (see Table 2), thus indicating that the influence of these two polar interactions in the binding is negligible with respect to the contribution of the sulfonamide binding and of the high number of van der Waals contacts established by the bulky organic scaffold.

Interestingly, the superposition of both hCA II/**30a** and hCA II/**30b** structures (see Figure 4A and Figure 4B) with that of the lead compound **3** in complex with the same enzyme[50] reveals that the

introduction of the C-1 phenyl substituent on the isoquinoline ring causes a dramatic rearrangement of the latter within the active site cavity. Indeed, such ring in the hCA II/**3** structure is located in the small hydrophobic pocket occupied by the phenyl ring in hCA II/**30a** and hCA II/**30b** adducts.

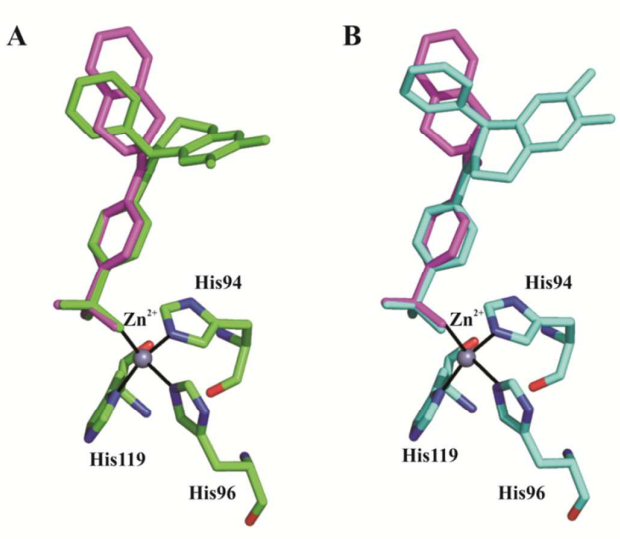

Figure 4. Structural superposition between (*R*)-**30a** and **3** (**A**) and (*S*)-**30b** and **3** (**B**) bound to the hCA II active site. **30a**, **30b** and **3** are colored in green, cyan and magenta respectively

These data suggest that the introduction of suitable substituents on the isoquinoline ring of compound **3** is a proper strategy to modulate the interactions of these inhibitors with different regions of the active site.

Molecular Modelling. To gain structural insights about the binding recognition into the catalytic pocket of hCA VII we performed molecular docking simulations selecting the structure of C183S/C217S mutant in complex with acetazolamide (PDB code 3ML5).[52] Specifically, we modelled the binding poses of derivatives (*R*)-**30a** and (*S*)-**30b** for which relevant and very similar inhibitory effects were found (K_i values of 0.21 and 0.19 nM, respectively).

Figure 5 displays the binding poses within hCA VII catalytic site for the inhibitors (*R*)-**30a** (pale green) and (*S*)-**30b** (orange). As found for the crystallographic structures of hCA II/**30a** and hCA

II/**30b** adducts, both (*R*)-**30a** and (*S*)-**30b** fit nicely the enzymatic pocket of hCA VII assuming two specular binding poses (Figure 5). In detail, the two arylsulfonamide moieties display similar binding orientation for which the deprotonated nitrogen atom coordinates the zinc ion within catalytic site. The C-1 phenyl substituents were buried in the hydrophobic cleft (area colored in red) defined by residues Phe131, Ala135, Leu 141, Leu198, Pro202, Leu204. Specifically, compound **30a** established van der Waals interactions with Phe131 generating a crucial T-shaped π-stacking; whereas for compound **30b** hydrophobic contact with Pro202 were found. The two isoquinoline rings are surrounded by the hydrophilic region (coloured area in blue) defined by residues Lys91, Asn62, His64, Thr199, Thr200 and the top portion of benzene-fused rings are exposed to solvent front (Figure 5). Moreover, enantiomer **30a** established an additional hydrogen bond interaction Lys91 through the 6-hydroxy-substituent.

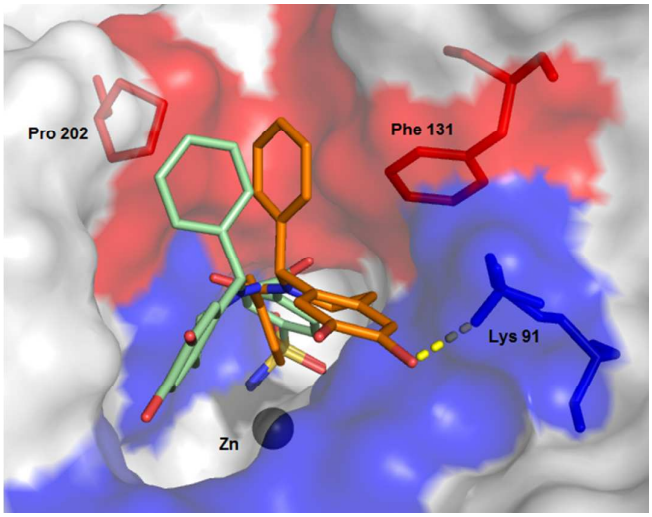

Figure 5. Compounds **30a** (orange) and **30b** (pale green) in stick representation docked into hCA VII active site; the hCA VII hydrophobic region is defined by residues Phe131 Ala135, Leu198, Pro202 (red); the hCA VII hydrophilic region is defined by residues Lys91, Asn62, His64, Thr199, Thr200 (blue). Active site residues involved in the interactions are also shown as sticks. Polar interaction is represented by yellow dotted lines. Zinc ion is represented by gray sphere.

To guide the design of further analogues and gain more information about isoform selectivity, we attempted to explain the slight difference of CA affinity of (*R*)-**30a** and (*S*)-**30b** toward hCA VII over hCA II (see Table 1). At this aim, the X-ray structures of hCA II/**30a** (5NOD) and hCA II/**30b** (5NOE) adducts were overlaid with the docking structures of the corresponding complexes with hCA VII (see Figure 6).

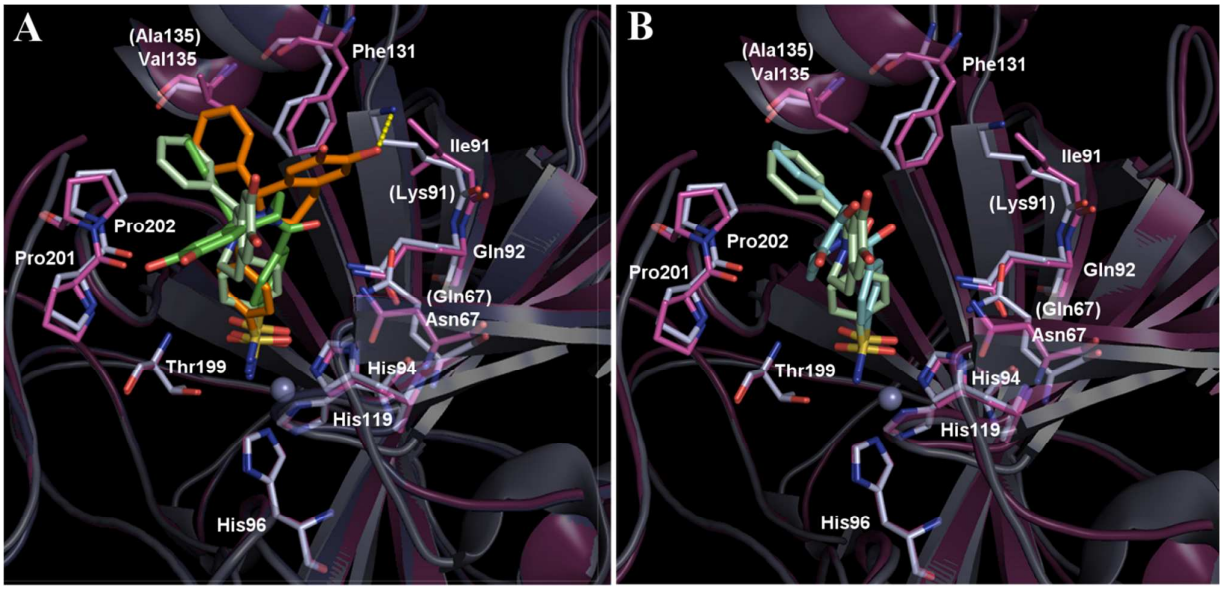

Figure 6. Comparison of binding modes for inhibitors **30a** and **30b** into active site cavities of hCA II (gray) and hCA VII (violet). (A) Docking pose of **30a** (orange) into hCA VII superimposed with its crystal structure in hCA II (green). (B) Docking pose of **30b** (pale green) into hCA VII superimposed with its crystal structure in hCA II (cyan). The Zinc ion is depicted as a gray sphere and dotted line indicates enzyme–ligand interaction. The not conserved residues in hCA VII are labeled in parentheses.

From the superposition it is evident that the (*S*)-enantiomer **30b** assumed a quite similar orientation in the active site of hCA VII and hCA II, whereas small differences were observed in the binding mode of (*R*)-**30a** to the two enzymes, particularly in the orientation of the dihydroxyisoquinoline ring. This moiety in hCA VII was oriented toward the hydrophilic pocket formed by residues Gln62, Gln67 and Lys91, establishing a hydrogen bond interaction with the polar residue Lys91,

which corresponds to the nonpolar residue of Ile91 of hCA II. Considering that the **30a** and **30b** share the same isoform selectivity profile, we can hypothesize that the hydrogen bond interaction with the residue Lys91 does not exert a crucial role for the affinity to hCA VII over hCA II. Overall, the lack of high isoform selectivity is probably due to the large hydrophobic/hydrophilic pocket that does not allow a good discrimination of each enantiomer for both enzymes for this class of isoquinolinesulfonamide inhibitors.

Conclusions

In this work we rationally designed and synthesized a new class of (*R,S*)-4-(1-aryl-3,4-dihydro-1*H*-isoquinoline-2-carbonyl)benzenesulfonamide derivatives (**23-33**) as CAIs. These compounds were designed by introducing additional hydrophobic/hydrophilic moieties on the known inhibitor **3** displaying low CA isoform selectivity. This approach proved to be efficacious to obtain new arylsulfonamides that proved to be active up to subnanomolar concentration. Specifically, the most active inhibitor **30** exerted excellent K_i value against hCA VII (0.20 nM). We carried out HPLC enantiomeric resolution and analyzed the proper binding position of the two enantiomers (*R*)-**30a** and (*S*)-**30b** into hCA II catalytic site. Moreover we docked (*R*)-**30a** and (*S*)-**30b** within hCA VII active site, thus obtaining insights into their binding positions. By collecting these structural studies, obtained by computational and experimental procedures, we confirmed that the presence of C-1 phenyl ring on isoquinoline ring of (*R,S*)-**30** generates extensive non-polar contacts within catalytic site. Overall, we have clearly demonstrated that highly potent CAIs should entirely occupy the two halves (hydrophilic and hydrophobic regions) of the catalytic site of hCA II/hCA VII isoforms.

Experimental section

Chemistry. Microwave-assisted reactions were carried out in a Focused Microwawe TM Synthesis System, Model Discover (CEM Technology Ltd Buckingham, UK). Melting points were determined on a Buchi B-545 apparatus (BUCHI Labortechnik AG Flawil, Switzerland) and are

uncorrected. By combustion analysis (C, H, N) carried out on a Carlo Erba Model 1106-Elemental Analyzer we determined the purity of synthesized compounds; the results confirmed a ≥95% purity. Merck Silica Gel 60 F254 plates were used for analytical TLC (Merck KGaA, Darmstadt, Germany,). Flash Chromatography (FC) was carried out on a Biotage SP1 EXP (Biotage AB Uppsala, Sweden). ^{1}H NMR spectra were measured in dimethylsulfoxide-d_6 (DMSO-d_6) with a Varian Gemini 300 spectrometer (Varian Inc. Palo Alto, California USA); chemical shifts are expressed in δ (ppm) and coupling constants (J) in hertz. All exchangeable protons were confirmed by addition of D_2O. R_f values were determined on TLC plates using a mixture of CH_2Cl_2/CH_3OH (96/4) as eluent.

General procedure for the synthesis of *(R,S)*-1-aryl-1,2,3,4-tetrahydroisoquinolines (17-22)

Following a previously reported procedure, the appropriate benzaldehyde (**7-10**) (1.2 mmol) and suitable phenylethylamine (**4-6**) (1.0 mmol,) were placed in a cylindrical quartz tube (Ø 2 cm), then stirred and irradiated in a microwave oven at 150W for 10 min at 90 °C. After cooling to room temperature, trifluoroacetic acid (3,3 ml) was added to crude intermediates **11-16** obtained in the previous step and the mixture was irradiated at 150W for 10 min at 90 °C. The reaction was basified (pH≅9) with sodium hydroxide, 10 N. The mixture was quenched by addition of H_2O (5 mL) and extracted with EtOAc (3 x 5 mL). The organic layer was dried over Na_2SO_4 and concentrated until dryness under reduced pressure. The crude product was collected by filtration and purified by crystallization with Et_2O and EtOH to afford compounds **17-22**. Analytical data for compounds **17, 19-22** are in good agreement with literature.[51, 53, 54]

1-Phenyl-6-propoxy-1,2,3,4-tetrahydroisoquinoline (18). Yield: 58%; M.p.:138-140°C; ^{1}HNMR (DMSO-d_6): δ 0.93 (t, 3H, CH_3, *J= 7.0*, *J= 7.6*), 1.66 (m, 2H, CH_2), 3.64- 3.06 (m, 4H, CH_2), 3.84 (t, 2H, CH_2, *J= 6.4*, *J= 6.5*), 4.88 (s, 1H, CH), 6.47 (d, *J= 8.2*, 1H, ArH), 6.55 (d, *J= 8.2*, 1H, ArH), 6.64 (s, 1H, ArH), 7.21-7.28 (m, 5H, ArH); Anal. Calcd for $C_{18}H_{21}NO$: C 80.86% H 7.92% N 5.24%; Found: C 80.96; H 7.83; N 5.16.

General procedure for the synthesis of 6/7-alkoxy-substituted derivatives of *(R,S)*-4-(1-aryl-3,4-dihydro-1*H*-isoquinoline-2-carbonyl)benzenesulfonamides (23-28)

To a solution of 4-(aminosulfonyl)benzoic acid (2 mmol) dissolved in dimethylformamide (DMF) (2mL) was added the N,N,N',N'-tetramethyl-O-(1H-benzotriazol-1-yl)-uraniumhexafluorophosphate (HBTU) (2 mmol). The mixture was stirred at room temperature for 1 h. Then TEA (2 mmol) and appropriate (*R,S*)-1-aryl-1,2,3,4-tetrahydroisoquinolines (**17-22**) (2 mmol) were added. The reaction mixture was left overnight at room temperature and then quenched with H_2O (10 mL) and extracted with EtOAc (3 x 5 mL). The organic phase was washed with an aqueous saturated solution of $NaHCO_3$ (2 x 5 mL), dried with Na_2SO_4 and concentrated until dryness under reduced pressure. The residue was purified by flash chromatography (DCM/MeOH 96:4), crystallized by treatment with Et_2O and EtOH to give the desired final compounds **23-28** as white crystals.

4-(6-Methoxy-1-phenyl-3,4-dihydro-1*H*-isoquinoline-2-carbonyl)benzenesulfonamide(23)

Yield: 31%; M.p.:239-241°C; R_f:0.36; ^{1}HNMR (DMSO-d_6): δ 2.71-3.38 (m, 4H, CH_2), 3.74 (s, 3H, OCH_3), 6.76 (s, 1H, CH), 6.81 (m, 2H, ArH), 7.05 (m, 1H, ArH), 7.24-7.33 (m, 5H, ArH), 7.46 (s, 2H, NH_2), 7.58 (d, *J= 8.2*, 2H, ArH); 7.87 (d, *J= 8.2*, 2H, ArH). Anal. Calcd for $C_{23}H_{22}N_2O_4S$: C 65.38%, H 5.25%, N 6.63%; Found: C 65.01, H 5.06, N 6.23.

4-(1-Phenyl-6-propoxy-3,4-dihydro-1*H*-isoquinoline-2-carbonyl)benzenesulfonamide (24)

Yield: 61%; M.p.:231-233°C; R_f:0.41; ^{1}HNMR (DMSO-d_6) δ 0.96 (t, 3H, *J= 7.0*, CH_3), 1.70-1.75 (m, 2H, CH_2), 2.69-2.94 (m, 4H, CH_2), 3.91 (t, 2H, *J= 6.5*, OCH_2), 6.76 (s, 1H, CH), 6.81 (m, 1H, ArH), 7.04-7.07 (m, 2H, ArH), 7.25-7.34 (m, 5H, ArH), 7.47 (s, 1H, NH_2), 7.59 (d, *J= 8.0*, 2H, ArH), 7.86 7.88 (d, *J= 8.0*, 2H, CH_2). Anal. Calcd for $C_{25}H_{26}N_2O_4S$: C 66.64%, H 5.82%, N 6.22%; Found: C 66.60, H 5.80, N 6.20.

4-(6,7-Dimethoxy-1-phenyl-3,4-dihydro-1*H*-isoquinoline-2-carbonyl)benzenesulfonamide (25)

Yield: 66%; Mp:248-250°C; R_f:0.41 ^{1}HNMR (DMSO-d_6): δ 2.63-3.25 (m, 4H, CH_2), 3.63 (s, 3H, OCH_3), 3.74 (s, 3H, OCH_3), 6.72 (s, 1H, CH), 6.78 (s, 1H, ArH), 6.80 (s, 1H, ArH), 7.22-7.34 (m,

5H, ArH), 7.46 (s, 2H, NH_2), 7.55 (d, *J= 8.2*, 2H, ArH), 7.85 (d, *J= 8.2*, 2H, ArH); Anal. Calcd for $C_{24}H_{24}N_2O_5S$: C 63.70%, H 5.35%, N 6.19%; Found: C 63.52, H 5.21, N 6.02.

4-[1-(4-Fluorophenyl)-6,7-dimethoxy-3,4-dihydro-1*H*-isoquinoline-2-carbonyl]benzenesulfonamide (26)

Yield: 41%; M.p.:220-222°C; R_f:0.47; ^{1}HNMR (DMSO-d_6) δ 2.63-3.40 (m, 4H, CH_2), 3.63 (s, 3H, OCH_3), 3.75 (s, 3H, OCH_3), 6.72 (s, 1H, CH), 6.78 (s, 1H, ArH), 6.81 (s, 1H, ArH), 7.14-7.27 (m, 4H, ArH), 7.46 (bs, 2H, NH_2), 7.57 (d, *J= 8.6*, 2H, ArH), 7.87 (d, *J= 8.6*, 2H, ArH); Anal. Calcd for $C_{24}H_{23}FN_2O_5S$: C 61.27%, H 4.93%, N 5.95%; Found: C 61.37, H 4.80, N 5.80.

4-[1-(4-Chlorophenyl)-6,7-dimethoxy-3,4-dihydro-1*H*-isoquinoline-2-carbonyl]benzenesulfonamide (27)

Yield: 50%; M.p.:204-205°C; R_f:0.40; ^{1}HNMR (DMSO-d_6) δ 2.64-3.23 (m, 4H, CH_2), 3.64 (s, 3H, OCH_3), 3.75 (s, 3H, OCH_3), 6.73 (s, 1H, CH), 6.77 (s, 1H, ArH), 6.81 (s, 1H, ArH), 7.28 (d, *J= 8.2*, 2H, ArH), 7.45 (bs, 2H, NH_2) 7.57 (d, *J= 8.2*, 2H, ArH), 7.87 (d, *J= 8.2*, 2H, ArH); Anal. Calcd for $C_{24}H_{23}ClN_2O_5S$: C 59.20%, H 4.76%, N 5.75%; Found: C 59.30, H 4.66, N 8.85.

4-[1-(4-Bromophenyl)-6,7-dimethoxy-3,4-dihydro-1*H*-isoquinoline-2-carbonyl]benzenesulfonamide (28)

Yield: 51%; M.p 191-192°C; R_f:0.41; ^{1}HNMR (DMSO-d_6) δ 2.63-3.38 (m, 4H, CH_2), 3.64 (s, 3H, OCH_3), 3.75 (s, 3H, OCH_3), 6.74 (m, 2H, ArH), 6.81 (s, 1H, CH), 7.19 (d, *J= 8.2*, 2H, ArH), 7.46 (bs, 2H, NH_2), 7.53-7.58 (m, 4H, ArH), 7.88 (d, *J= 7.6*, 2H, ArH). Anal. Calcd for $C_{24}H_{23}BrN_2O_5S$: C 54.24%, H 4.36%, N 5.27%; Found: C 54.34, H 4.46, N 5.20.

General procedure for the synthesis of 6/7-hydroxy-substituted derivatives of *(R,S)*-4-(1-aryl-3,4-dihydro-1*H*-isoquinoline-2-carbonyl)benzenesulfonamides (29-33)

The methoxy-derivatives **23, 25-28** (1 mmol) were dissolved in methylene chloride (DCM) (5 mL), treated with BBr_3 (1M in DCM) (6 mmol) under nitrogen atmosphere and stirred overnight. After completion of the reaction, MeOH (7 mL) was carefully added at 0°C and the solvents removed

under reduced pressure. The residue was dissolved in EtOAc (10 mL) and washed with H_2O (3 x 10 mL). The organic layer was dried (Na_2SO_4) and concentrated in vacuo. The crude products were crystallized from Et_2O to give the desired corresponding hydroxy-derivatives **29-33**.

4-(6-Hydroxy-1-phenyl-3,4-dihydro-1*H*-isoquinoline-2-carbonyl)benzenesulfonamide (29)

Yield: 86%; Mp: 282-284°C; R_f:0.23; ^{1}HNMR (DMSO-d_6): δ 2.62-3.39 (m, 4H, CH_2), 6.62 (s, 1H, ArH), 6.72 (s, 1H, CH), 6.93 (m, 1H, ArH), 7.22 (d, 1H, ArH), 7.25-7.34 (m, 5H, ArH), 7.46 (s, 2H, NH_2), 7.58 (d, *J*= 8.2, 2H, ArH), 7.87 (d, *J*=8.2, 2H, ArH), 9.42 (bs, 1H, OH). Anal. Calcd for $C_{22}H_{20}N_2O_4S$: C 64.69%, H 4.94%, N 6.86%; Found: C 64.49, H 4.65, N 6.75.

4-(6,7-Dihydroxy-1-phenyl-3,4-dihydro-1*H*-isoquinoline-2-carbonyl)benzenesulfonamide (30)

Yield: 83%; Mp: 239-240°C; R_f: 0.10; ^{1}HNMR (DMSO-d_6): δ 2.71-3.28 (m, 4H, CH_2), 6.41 (s, 1H, CH), 6.57 (s, 1H, ArH), 6.60 (s, 1H, ArH), 7.24-7.33 (m, 5H, ArH), 7.46 (s, 2H, NH_2), 7.54 (d, *J*= *8.2*, 2H, ArH), 7.85 (d, *J*= *8.2*, 2H, ArH), 8.86 (s, 1H, OH), 8.95 (s, 1H, OH). Anal. Calcd for $C_{22}H_{20}N_2O_5S$: C 62.25%, H 4.75%, N 6.60%; Found: C 62.01, H 4.45, N 6.52.

4-[6,7-Dihydroxy-1-(4-fluorophenyl)-3,4-dihydro-1*H*-isoquinoline-2-carbonyl]benzenesulfonamide (31)

Yield: 31%; M.p.:240-243°C; R_f: 0.11; ^{1}HNMR (DMSO-d_6) δ 2.57-3.23 (m, 4H, CH_2), 3.64 (s, 3H, OCH_3), 3.76 (s, 3H, OCH_3), 6.82 (s, 1H, CH), 6.85 (s, 1H, ArH), 6.88 (s, 1H, ArH), 7.47 (bs, 2H, NH_2), 7.58-7.70 (m, 4H, ArH), 7.88 (d, *J*= *8.2*, 2H, ArH), 8.07 (s, 1H, ArH); 8.16 (m, 1H,ArH). Anal. Calcd for $C_{24}H_{23}N_3O_7S$: C 57.94%, H 4.66%, N 8.45%; Found: C 57.84, H 4.76, N 8.55.

4-[1-(4-Chlorophenyl)-6,7-dihydroxy-3,4-dihydro-1*H*-isoquinoline-2-carbonyl]benzenesulfonamide (32)

Yield: 67%; M.p.:185-186°C; R_f: 0.12; ^{1}HNMR (DMSO-d_6) δ 2.42-3.23 (m, 4H, CH_2), 6.42 (s, 1H, CH), 6.57-6.58 (m, 2H, ArH), 7.27 (d, *J*= *8.2*, 2H, ArH), 7.40 (d, *J*= *8.2*, 2H, ArH), 7.46 (bs, 2H, NH_2) 7.55 (d, *J*= *8.2*, 2H, ArH), 7.85 (d, *J*= *8.2*, 2H, ArH), 8.88 (bs, 1H, OH), 8.98 (bs, 1H, OH). Anal. Calcd for $C_{22}H_{19}ClN_2O_5S$: C 57.58%, H 4.17%, N 6.10%; Found: C 57.68, H 4.10, N 6.20.

4-[1-(4-Bromophenyl)-6,7-dihydroxy-3,4-dihydro-1*H*-isoquinoline-2-carbonyl]benzenesulfonamide (33)

Yield: 42%; M.p.:189-191°C; R_f:0.13; ^{1}HNMR (DMSO-d_6) δ 2.07 (m, 4H, CH_2), 6.41 (s, 1H, CH), 6.57 (s, 2H, ArH), 7.20 (d, *J*= *8.3*, 2H, ArH), 7.46 (bs, 2H, NH_2), 7.52-7.56 (m, 4H, ArH), 7.85 (d, *J*= *8.3*, 2H, ArH), 9.00 (bs, 2H, OH). Anal. Calcd for $C_{22}H_{19}BrN_2O_5S$: C 52.49%, H 3.80%, N 5.57%; Found: C 52.52, H 3.84, N 5.60.

CA Inhibition Assay An Applied Photophysics stopped-flow instrument has been used for assaying the CA catalysed CO_2 hydration activity. Phenol red (at a concentration of 0.2 mM) has been used as indicator, working at the absorbance maximum of 557 nm, with 10 – 20 mM Hepes (pH 7.5) or Tris (pH 8.3) as buffers, and 20 mM Na_2SO_4 or 20 mM $NaClO_4$ (for maintaining constant the ionic strength), following the initial rates of the CA-catalyzed CO_2 hydration reaction for a period of 10-100 s. The CO_2 concentrations ranged from 1.7 to 17 mM for the determination of the kinetic parameters and inhibition constants. For each inhibitor at least six traces of the initial 5-10% of the reaction have been used for determining the initial velocity. The uncatalyzed rates were determined in the same manner and subtracted from the total observed rates. Stock solutions of inhibitor (10 mM) were prepared in distilled-deionized water and dilutions up to 0.01 nM were done thereafter with distilled-deionized water. Inhibitor and enzyme solutions were preincubated together for 15 min at room temperature prior to assay, in order to allow for the formation of the E-I complex. The inhibition constants were obtained by non-linear least-squares methods using PRISM 3, as reported earlier, and represent the mean from at least three different determinations. CA isoforms were recombinant ones obtained as reported earlier by this group.[55-57]

Enantiomeric resolution. Enantioselective HPLC analyses were performed by using stainless-steel Chiralpak IA (250 mm x 4.6 mm I.D. and 250 mm x 10 mm I.D.) and Chiralpak AS-H (250 mm x 4.6 mm I.D. and 250 mm x 10 mm I.D.) (Daicel, Chemical Industries, Tokyo, Japan) columns. HPLC-grade solvents were used as supplied by Aldrich (Milan, Italy). The HPLC apparatus

consisted of a Perkin Elmer (Norwalk, CT, USA) 200 lc pump equipped with a Rheodyne (Cotati, CA, USA) injector, a 1000-μl sample loop, a HPLC Perkin Elmer oven and a Perkin Elmer 290 detector. The signal was acquired and processed by Clarity software (DataApex, Prague, The Czech Republic). HPLC resolutions were carried out by using polysaccharide-based chiral stationary phases (CSPs). The CD spectra of the enantiomers isolated at semipreparative scale, dissolved in dichloromethane (concentration about 0.2 mg/ml) in a quartz cell (0.1 cm-path length) at 25 °C, were measured by using a Jasco (Jasco, Ishikawa-cho, Hachioji City, Tokyo, Japan) Model J-700 spectropolarimeter in the 400-200 nm spectral range. The spectra are average computed over three instrumental scans and the intensities are presented in terms of terms of ellipticity values (mdeg).

X-ray crystallography. Crystals of hCA II adducts with inhibitors (*R*)-**30a** and (*S*)-**30b** were prepared by the soaking technique. In particular, hCA II native crystals were grown at room temperature using the vapor diffusion hanging drop method. Equal volumes of protein (10 mg/ml in 0.02 M Tris-HCl pH 8.0) and precipitant solutions (1.3 M sodium citrate and 0.1 M Tris-HCl, pH 8.5) were mixed and equilibrated against 1 mL reservoir containing the same precipitant solution. A few native enzyme crystals were then transferred in a 3 μl drop of freshly prepared precipitant solution, containing 10% (v/v) glycerol and 20 mM inhibitor. These crystals were kept in the soaking solution for about 12 hours. Crystals were frozen in a gaseous nitrogen stream prior to the diffraction experiment. Complete X-ray data set were collected at 100 K by a copper rotating anode generator developed by Rigaku and equipped with a Rigaku Saturn CCD detector. Diffraction data up to 1.70 Å resolution for **hCA II/30a** and 1.75 Å resolution for **hCA II/30b** were processed and scaled using program HKL2000 (HKL Research).[58] Data collection statistics are reported in Table 1S. The initial phases of hCA II/inhibitor structures were calculated using the atomic coordinates of the native enzyme with waters removed (PDB entry 1CA2).[59] Clear electron density for the two compounds was observed in the difference maps after a single round of refinement. A model for both **30a** and **30b** was then built and introduced into the atomic coordinates set for further refinement, which proceeded to convergence with alternating cycles of water addiction, manual

rebuilding with the O program,[60] and energy minimization and B-factor refinement with the CNS program.[61] Crystallographic refinement was carried out against 95% of the measured data. The remaining 5% of the observed data, which was randomly selected, was used for Rfree calculations to monitor the progress of refinement. Topology files for both compounds were obtained using the PRODRG server.[62] The final R-work and R-free values were 0.173 and 0.209 for hCA II/**30a** and 0.166 and 0.198 for hCA II/**30b**. Refinement statistics are summarized in Table 1S (see Supporting Information). Coordinates and structure factors have been deposited in the Protein Data Bank (accession codes 5NOD and 5NOE).

Molecular docking. The crystal structures of hCA VII in complex with the inhibitor acetazolamide was retrieved from the RCSB Protein Data Bank (PDB: 3ML5).[52] Ligand and water molecules were discarded, and hydrogen atoms were added to protein with Discovery Studio 2.5.5.[63] Structures of the ligands were constructed using Discovery Studio 2.5.5 and energy minimized using the Smart Minimizer protocol (1000 steps) which combines the Steepest Descent and the Conjugate Gradient methods. The ligands minimized in this way were docked in their corresponding proteins by means of Gold Suite 5.0.1.[64] The region of interest used by Gold program was defined in order to contain residues within 10 Å from the original position of the ligand in the X-ray structure. A scaffold constraint (penalty = 10.0) was used to restrict the solutions in which the sulfonamide moiety was able to coordinate the metal within the catalytic binding site. GoldScore was chosen as fitness function, the standard default setting was used in all calculations and ligands were submitted to 100 genetic algorithm runs. The "allow early termination" command was deactivated. Results differing by less than 0.75 Å in ligand-all atom RMSD, were clustered together. The best GOLD-calculated conformation was used both for analysis and representation.

Acknowledgments

Financial support for this research by by Fondo di Ateneo per la Ricerca (PRA grant number ORME09SPNC - Università degli Studi di Messina)

Associated content

Supporting Information. The Supporting Information is available free of charge on the ACS Publications website at DOI:

Diffraction Data and Refinement Statistics, CD spectra of the enantiomers (PDF)

Molecular formula strings (XLSX)

Accession Codes. The final models of hCA II bound to inhibitors **30a** and **30b** are deposited to the Protein Databank (5NOD and 5NOE). Authors will release the atomic coordinates and experimental data upon article publication

Author information

Corresponding author: Rosaria Gitto, PhD, Associate professor on Medicinal Chemistry, Dipartimento Scienze Chimiche, Biologiche, Farmaceutiche ed Ambientali (CHIBIOFARAM), Università degli Studi di Messina, Viale Annunziata, I-98168, Messina. Tel 00390906766413, Fax 00390906766404, e-mail: rgitto@unime.it ORCID: Gitto Rosaria 0000-0003-0002-2253

Author Contributions: The manuscript was written through contributions of all authors.

Notes The authors declare no competing financial interest.

Abbreviation Used

AAZ acetazolamide

CA carbonic anhydrase

CSPS chiral stationary phases

DCM dichloromethane

FC Flash Chromatography

HBTU ***N,N,N′,N′***-Tetramethyl-*O*-(1*H*-benzotriazol-1-yl)uronium hexafluorophosphate

MW Microwave

TEA triethylamine

TFA Trifluoroacetic acid

TLC Thin Layer Chromatography

TPM topiramate

References

1. Supuran, C. T. Diuretics: from classical carbonic anhydrase inhibitors to novel applications of the sulfonamides. *Curr. Pharm. Des.* **2008,** *14*, 641-648.

2. Mincione, F.; Scozzafava, A.; Supuran, C. T. The development of topically acting carbonic anhydrase inhibitors as antiglaucoma agents. *Curr. Pharm. Des.* **2008,** *14*, 649-654.

3. De Simone, G.; Di Fiore, A.; Supuran, C. T. Are carbonic anhydrase inhibitors suitable for obtaining antiobesity drugs? *Curr. Pharm. Des.* **2008,** *14*, 655-660.

4. Thiry, A.; Dogne, J. M.; Supuran, C. T.; Masereel, B. Carbonic anhydrase inhibitors as anticonvulsant agents. *Curr. Top. Med. Chem.* **2007,** *7*, 855-864.

5. Supuran, C. T. Inhibition of bacterial carbonic anhydrases and zinc proteases: from orphan targets to innovative new antibiotic drugs. *Curr. Med. Chem.* **2012,** *19*, 831-844.

6. Bao, B.; Groves, K.; Zhang, J.; Handy, E.; Kennedy, P.; Cuneo, G.; Supuran, C. T.; Yared, W.; Rajopadhye, M.; Peterson, J. D. In vivo imaging and quantification of carbonic anhydrase IX expression as an endogenous biomarker of tumor hypoxia. *PLoS One* **2012,** *7*, e50860.

7. Supuran, C. T. Carbonic anhydrase inhibitors as emerging drugs for the treatment of obesity. *Expert Opin. Emerg. Drugs* **2012,** *17*, 11-15.

8. Supuran, C. T. Carbonic anhydrases: novel therapeutic applications for inhibitors and activators. *Nat. Rev. Drug Discov.* **2008,** *7*, 168-181.

9. Thiry, A.; Masereel, B.; Dogne, J. M.; Supuran, C. T.; Wouters, J.; Michaux, C. Exploration of the binding mode of indanesulfonamides as selective inhibitors of human carbonic anhydrase type VII by targeting Lys 91. *ChemMedChem* **2007,** *2*, 1273-1280.

10. De Simone, G.; Scozzafava, A.; Supuran, C. T. Which carbonic anhydrases are targeted by the antiepileptic sulfonamides and sulfamates? *Chem. Biol. Drug Des.* **2009,** *74*, 317-321.

11. Monti, S. M.; Supuran, C. T.; De Simone, G. Carbonic anhydrase IX as a target for designing novel anticancer drugs. *Curr. Med. Chem.* **2012,** *19*, 821-830.

12. Nishimori, I.; Vullo, D.; Minakuchi, T.; Scozzafava, A.; Capasso, C.; Supuran, C. T. Restoring catalytic activity to the human carbonic anhydrase (CA) related proteins VIII, X and XI affords isoforms with high catalytic efficiency and susceptibility to anion inhibition. *Bioorg. Med. Chem. Lett.* **2013,** *23*, 256-260.

13. Said, H. M.; Supuran, C. T.; Hageman, C.; Staab, A.; Polat, B.; Katzer, A.; Scozzafava, A.; Anacker, J.; Flentje, M.; Vordermark, D. Modulation of carbonic anhydrase 9 (CA9) in human brain cancer. *Curr. Pharm. Des.* **2010,** *16*, 3288-3299.

14. Guler, O. O.; De Simone, G.; Supuran, C. T. Drug design studies of the novel antitumor targets carbonic anhydrase IX and XII. *Curr. Med. Chem.* **2010,** *17*, 1516-1526.

15. Akurathi, V.; Dubois, L.; Lieuwes, N. G.; Chitneni, S. K.; Cleynhens, B. J.; Vullo, D.; Supuran, C. T.; Verbruggen, A. M.; Lambin, P.; Bormans, G. M. Synthesis and biological evaluation of a 99mTc-labelled sulfonamide conjugate for in vivo visualization of carbonic anhydrase IX expression in tumor hypoxia. *Nucl. Med. Biol.* **2010,** *37*, 557-564.

16. Genis, C.; Sippel, K. H.; Case, N.; Cao, W.; Avvaru, B. S.; Tartaglia, L. J.; Govindasamy, L.; Tu, C.; Agbandje-McKenna, M.; Silverman, D. N.; Rosser, C. J.; McKenna, R. Design of a

carbonic anhydrase IX active-site mimic to screen inhibitors for possible anticancer properties. *Biochemistry* **2009,** *48*, 1322-1331.

17. Thiry, A.; Supuran, C. T.; Masereel, B.; Dogne, J. M. Recent developments of carbonic anhydrase inhibitors as potential anticancer drugs. *J. Med. Chem.* **2008,** *51*, 3051-3056.

18. Pastorekova, S.; Kopacek, J.; Pastorek, J. Carbonic anhydrase inhibitors and the management of cancer. *Curr. Top. Med. Chem.* **2007,** *7*, 865-878.

19. De Simone, G.; Vitale, R. M.; Di Fiore, A.; Pedone, C.; Scozzafava, A.; Montero, J. L.; Winum, J. Y.; Supuran, C. T. Carbonic anhydrase inhibitors: hypoxia-activatable sulfonamides incorporating disulfide bonds that target the tumor-associated isoform IX. *J. Med. Chem.* **2006,** *49*, 5544-5551.

20. Meijer, T. W.; Bussink, J.; Zatovicova, M.; Span, P. N.; Lok, J.; Supuran, C. T.; Kaanders, J. H. Tumor microenvironmental changes induced by the sulfamate carbonic anhydrase IX inhibitor S4 in a laryngeal tumor model. *PLoS One* **2014,** *9*, e108068.

21. Krall, N.; Pretto, F.; Decurtins, W.; Bernardes, G. J.; Supuran, C. T.; Neri, D. A small-molecule drug conjugate for the treatment of carbonic anhydrase IX expressing tumors. *Angew. Chem. Int. Ed. Engl.* **2014,** *53*, 4231-4235.

22. Monti, S. M.; Supuran, C. T.; De Simone, G. Anticancer carbonic anhydrase inhibitors: a patent review (2008 - 2013). *Exp. Opin. Ther. Patents* **2013,** *23*, 737-749.

23. Parkkila, S.; Parkkila, A. K.; Rajaniemi, H.; Shah, G. N.; Grubb, J. H.; Waheed, A.; Sly, W. S. Expression of membrane-associated carbonic anhydrase XIV on neurons and axons in mouse and human brain. *Proc. Natl .Acad. Sci. U.S.A.* **2001,** *98*, 1918-1923.

24. Alterio, V.; Pan, P.; Parkkila, S.; Buonanno, M.; Supuran, C. T.; Monti, S. M.; De Simone, G. The structural comparison between membrane-associated human carbonic anhydrases provides insights into drug design of selective inhibitors. *Biopolymers* **2014,** *101*, 769-778.

25. Alterio, V.; Di Fiore, A.; D'Ambrosio, K.; Supuran, C. T.; De Simone, G. Multiple binding modes of inhibitors to carbonic anhydrases: how to design specific drugs targeting 15 different isoforms? *Chem. Rev.* **2012,** *112*, 4421-4468.

26. Carta, F.; Scozzafava, A.; Supuran, C. T. Sulfonamides: a patent review (2008 - 2012). *Expert Opin. Ther. Pat.* **2012,** *22*, 747-758.

27. D'Ambrosio, K.; Smaine, F. Z.; Carta, F.; De Simone, G.; Winum, J. Y.; Supuran, C. T. Development of potent carbonic anhydrase inhibitors incorporating both sulfonamide and sulfamide groups. *J. Med. Chem.* **2012,** *55*, 6776-6783.

28. Marini, A. M.; Maresca, A.; Aggarwal, M.; Orlandini, E.; Nencetti, S.; Da Settimo, F.; Salerno, S.; Simorini, F.; La Motta, C.; Taliani, S.; Nuti, E.; Scozzafava, A.; McKenna, R.; Rossello, A.; Supuran, C. T. Tricyclic sulfonamides incorporating benzothiopyrano[4,3-c]pyrazole and pyridothiopyrano[4,3-c]pyrazole effectively inhibit alpha- and beta-carbonic anhydrase: X-ray crystallography and solution investigations on 15 isoforms. *J. Med. Chem.* **2012,** *55*, 9619-9629.

29. Supuran, C. T. Carbonic anhydrase inhibitors. *Bioorg. Med. Chem. Lett.* **2010,** *20*, 3467-3474.

30. Supuran, C. T. Carbonic anhydrases: again, and again, and again. *Curr. Pharm. Des.* **2010,** *16*, 3231-3232.

31. Supuran, C. T. Carbonic anhydrase inhibition/activation: trip of a scientist around the world in the search of novel chemotypes and drug targets. *Curr. Pharm. Des.* **2010,** *16*, 3233-3245.

32. Schulze Wischeler, J.; Innocenti, A.; Vullo, D.; Agrawal, A.; Cohen, S. M.; Heine, A.; Supuran, C. T.; Klebe, G. Bidentate Zinc chelators for alpha-carbonic anhydrases that produce a trigonal bipyramidal coordination geometry. *ChemMedChem* **2010,** *5*, 1609-1615.

33. Winum, J. Y.; Scozzafava, A.; Montero, J. L.; Supuran, C. T. Therapeutic potential of sulfamides as enzyme inhibitors. *Med. Res. Rev.* **2006, 26**, 767-792.

34. Winum, J. Y.; Scozzafava, A.; Montero, J. L.; Supuran, C. T. Sulfamates and their therapeutic potential. *Med. Res. Rev.* **2005,** *25*, 186-228.

35. Pala, N.; Micheletto, L.; Sechi, M.; Aggarwal, M.; Carta, F.; McKenna, R.; Supuran, C. T. Carbonic anhydrase inhibition with benzenesulfonamides and tetrafluorobenzenesulfonamides obtained via click chemistry. *ACS Med. Chem. Lett.* **2014,** *5*, 927-930.

36. Carta, F.; Supuran, C. T.; Scozzafava, A. Sulfonamides and their isosters as carbonic anhydrase inhibitors. *Future Med. Chem.* **2014,** *6*, 1149-1165.

37. Gitto, R.; Agnello, S.; Ferro, S.; De Luca, L.; Vullo, D.; Brynda, J.; Mader, P.; Supuran, C. T.; Chimirri, A. Identification of 3,4-Dihydroisoquinoline-2(1H)-sulfonamides as potent carbonic anhydrase inhibitors: synthesis, biological evaluation, and enzyme--ligand X-ray studies. *J. Med. Chem.* **2010,** *53*, 2401-2408.

38. Mader, P.; Brynda, J.; Gitto, R.; Agnello, S.; Pachl, P.; Supuran, C. T.; Chimirri, A.; Rezacova, P. Structural basis for the interaction between carbonic anhydrase and 1,2,3,4-tetrahydroisoquinolin-2-ylsulfonamides. *J. Med. Chem.* **2011,** *54*, 2522-2526.

39. Gitto, R.; Agnello, S.; Ferro, S.; Vullo, D.; Supuran, C. T.; Chimirri, A. Identification of potent and selective human carbonic anhydrase VII (hCA VII) inhibitors. *ChemMedChem* **2010,** *5*, 823-826.

40. Alterio, V.; Di Fiore, A.; D'Ambrosio, K.; Supuran, C. T.; De Simone, G. Multiple binding modes of inhibitors to carbonic anhydrases: how to design specific drugs targeting 15 different isoforms? *Chem. Rev.* **2012,** *112*, 4421-4468.

41. Vullo, D.; Supuran, C. T.; Scozzafava, A.; De Simone, G.; Monti, S. M.; Alterio, V.; Carta, F. Kinetic and X-ray crystallographic investigations of substituted 2-thio-6-oxo-1,6-dihydropyrimidine-benzenesulfonamides acting as carbonic anhydrase inhibitors. *Bioorg. Med. Chem.* **2016,** *24*, 3643-3648.

42. Fisher, S. Z.; Govindasamy, L.; Boyle, N.; Agbandje-McKenna, M.; Silverman, D. N.; Blackburn, G. M.; McKenna, R. X-ray crystallographic studies reveal that the incorporation of spacer groups in carbonic anhydrase inhibitors causes alternate binding modes. *Acta Crystallogr. Sect. F Struc.t Biol .Cryst. Commun.* **2006,** *62*, 618-622.

43. Alterio, V.; Vitale, R. M.; Monti, S. M.; Pedone, C.; Scozzafava, A.; Cecchi, A.; De Simone, G.; Supuran, C. T. Carbonic anhydrase inhibitors: X-ray and molecular modeling study for the interaction of a fluorescent antitumor sulfonamide with isozyme II and IX. *J. Am. Chem. Soc.* **2006,** *128*, 8329-8335.

44. Menchise, V.; De Simone, G.; Alterio, V.; Di Fiore, A.; Pedone, C.; Scozzafava, A.; Supuran, C. T. Carbonic anhydrase inhibitors: stacking with Phe131 determines active site binding region of inhibitors as exemplified by the X-ray crystal structure of a membrane-impermeant antitumor sulfonamide complexed with isozyme II. *J. Med. Chem.* **2005,** *48*, 5721-5727.

45. Bozdag, M.; Ferraroni, M.; Nuti, E.; Vullo, D.; Rossello, A.; Carta, F.; Scozzafava, A.; Supuran, C. T. Combining the tail and the ring approaches for obtaining potent and isoform-selective carbonic anhydrase inhibitors: solution and X-ray crystallographic studies. *Bioorg. Med. Chem.* **2014,** *22*, 334-340.

46. Di Fiore, A.; Monti, S. M.; Hilvo, M.; Parkkila, S.; Romano, V.; Scaloni, A.; Pedone, C.; Scozzafava, A.; Supuran, C. T.; De Simone, G. Crystal structure of human carbonic anhydrase XIII and its complex with the inhibitor acetazolamide. *Proteins* **2009,** *74*, 164-175.

47. Alterio, V.; Hilvo, M.; Di Fiore, A.; Supuran, C. T.; Pan, P.; Parkkila, S.; Scaloni, A.; Pastorek, J.; Pastorekova, S.; Pedone, C.; Scozzafava, A.; Monti, S. M.; De Simone, G. Crystal structure of the catalytic domain of the tumor-associated human carbonic anhydrase IX. *Proc. Natl. Acad. Sci. U.S.A.* **2009,** *106*, 16233-16238.

48. Moeker, J.; Mahon, B. P.; Bornaghi, L. F.; Vullo, D.; Supuran, C. T.; McKenna, R.; Poulsen, S. A. Structural insights into carbonic anhydrase IX isoform specificity of carbohydrate-based sulfamates. *J. Med. Chem.* **2014**, *57,* 8635-8645.

49. De Simone, G.; Pizika, G.; Monti, S. M.; Di Fiore, A.; Ivanova, J.; Vozny, I.; Trapencieris, P.; Zalubovskis, R.; Supuran, C. T.; Alterio, V. Hydrophobic substituents of the phenylmethylsulfamide moiety can be used for the development of new selective carbonic anhydrase inhibitors. *Biomed. Res. Int.* **2014,** *2014*, 523210.

50. Buemi, M. R.; De Luca, L.; Ferro, S.; Bruno, E.; Ceruso, M.; Supuran, C. T.; Pospíšilová, K.; Brynda, J.; Řezáčová, P.; Gitto, R. Carbonic anhydrase inhibitors: Design, synthesis and structural characterization of new heteroaryl-N-carbonylbenzenesulfonamides targeting druggable human carbonic anhydrase isoforms. *Eur. J. Med. Chem.* **2015,** *102*, 223-232.

51. Gitto, R.; Damiano, F. M.; De Luca, L.; Ferro, S.; Vullo, D.; Supuran, C. T.; Chimirri, A. Synthesis and biological profile of new 1,2,3,4-tetrahydroisoquinolines as selective carbonic anhydrase inhibitors. *Bioorg. Med. Chem.* **2011,** *19*, 7003-7007.

52. Di Fiore, A.; Truppo, E.; Supuran, C. T.; Alterio, V.; Dathan, N.; Bootorabi, F.; Parkkila, S.; Monti, S. M.; De Simone, G. Crystal structure of the C183S/C217S mutant of human CA VII in complex with acetazolamide. *Bioorg. Med. Chem. Lett.* **2010,** *20*, 5023-5026.

53. Gitto, R.; Ficarra, R.; Stancanelli, R.; Guardo, M.; De Luca, L.; Barreca, M. L.; Pagano, B.; Rotondo, A.; Bruno, G.; Russo, E.; De Sarro, G.; Chimirri, A. Synthesis, resolution, stereochemistry, and molecular modeling of (R)- and (S)-2-acetyl-1-(4'-chlorophenyl)-6,7-dimethoxy-1,2,3,4-tetrahydroisoquinoline AMPAR antagonists. *Bioorg. Med. Chem.* **2007,** *15*, 5417-5423.

54. Gitto, R.; Ferro, S.; Agnello, S.; De Luca, L.; De Sarro, G.; Russo, E.; Vullo, D.; Supuran, C. T.; Chimirri, A. Synthesis and evaluation of pharmacological profile of 1-aryl-6,7-dimethoxy-3,4-dihydroisoquinoline-2(1H)-sulfonamides. *Bioorg. Med. Chem.* **2009,** *17*, 3659-3664.

55. Innocenti, A.; Vullo, D.; Pastorek, J.; Scozzafava, A.; Pastorekova, S.; Nishimori, I.; Supuran, C. T. Carbonic anhydrase inhibitors. Inhibition of transmembrane isozymes XII (cancer-associated) and XIV with anions. *Bioorg. Med. Chem. Lett.* **2007,** *17*, 1532-1537.

56. Nishimori, I.; Vullo, D.; Innocenti, A.; Scozzafava, A.; Mastrolorenzo, A.; Supuran, C. T. Carbonic anhydrase inhibitors: inhibition of the transmembrane isozyme XIV with sulfonamides. *Bioorg. Med. Chem. Lett.* **2005,** *15*, 3828-3833.

57. Nishimori, I.; Vullo, D.; Innocenti, A.; Scozzafava, A.; Mastrolorenzo, A.; Supuran, C. T. Carbonic anhydrase inhibitors. The mitochondrial isozyme VB as a new target for sulfonamide and sulfamate inhibitors. *J. Med. Chem.* **2005,** *48*, 7860-7866.

58. Otwinowski, Z., Minor, W. Processing of X-ray diffraction data collected in oscillation mode. *Methods Enzymol.* **1997,** *276*, 307-326.

59. Eriksson, A. E.; Jones, T. A.; Liljas, A. Refined structure of human carbonic anhydrase II at 2.0 A resolution. *Proteins* **1988,** 4, 274-282.

60. Jones, T. A.; Zou, J. Y.; Cowan, S. W.; Kjeldgaard, M. Improved methods for building protein models in electron density maps and the location of errors in these models. *Acta Crystallogr. Sect. A, Found. Crystallogr.* **1991,** *47* (Pt 2), 110-119.

61. Brunger, A. T. Version 1.2 of the Crystallography and NMR system. *Nat. Protoc.* **2007,** *2*, 2728-2733.

62. Schuttelkopf, A. W.; van Aalten, D. M. PRODRG: a tool for high-throughput crystallography of protein-ligand complexes. *Acta Crystallogr. Sect. D, Biol .Cryst.* **2004,** *60*, 1355-1363.

63. *Discovery Studio* 2.5.5; Accelrys, http://www.accelrys.com: San Diego, CA USA, 2009.

64. Jones, G.; Willett, P.; Glen, R. C.; Leach, A. R.; Taylor, R. Development and validation of a genetic algorithm for flexible docking. *J. Mol. Biol.* **1997,** *267*, 727-748.

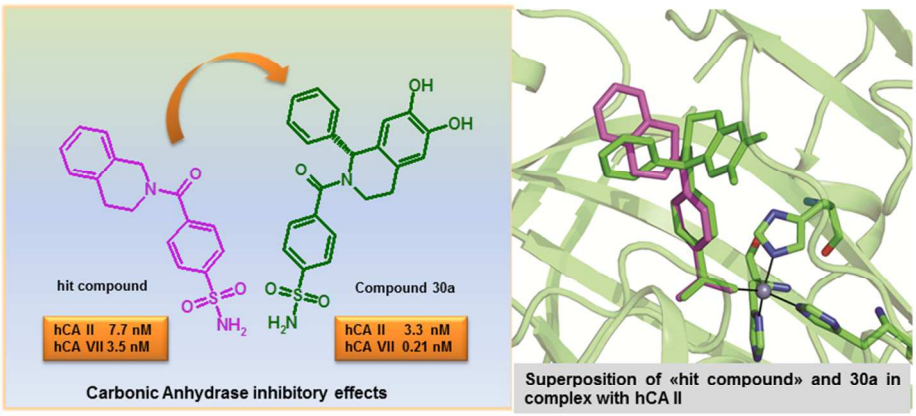

Table of Content Graphic

254x190mm (96 x 96 DPI)

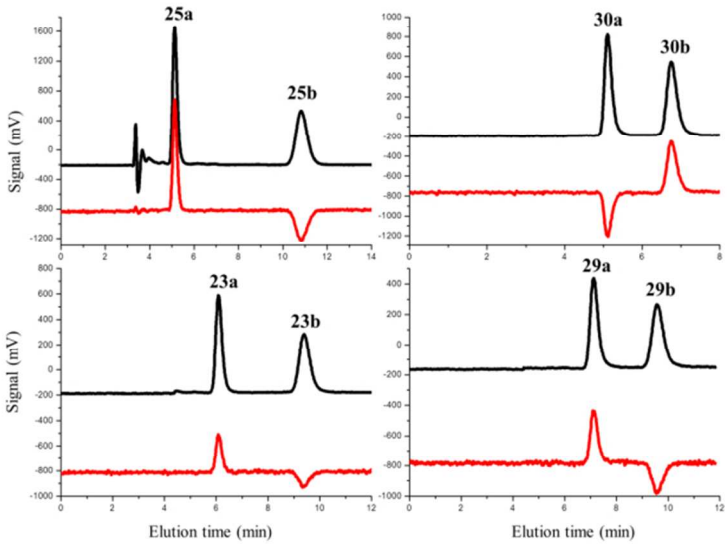

97x73mm (220 x 220 DPI)

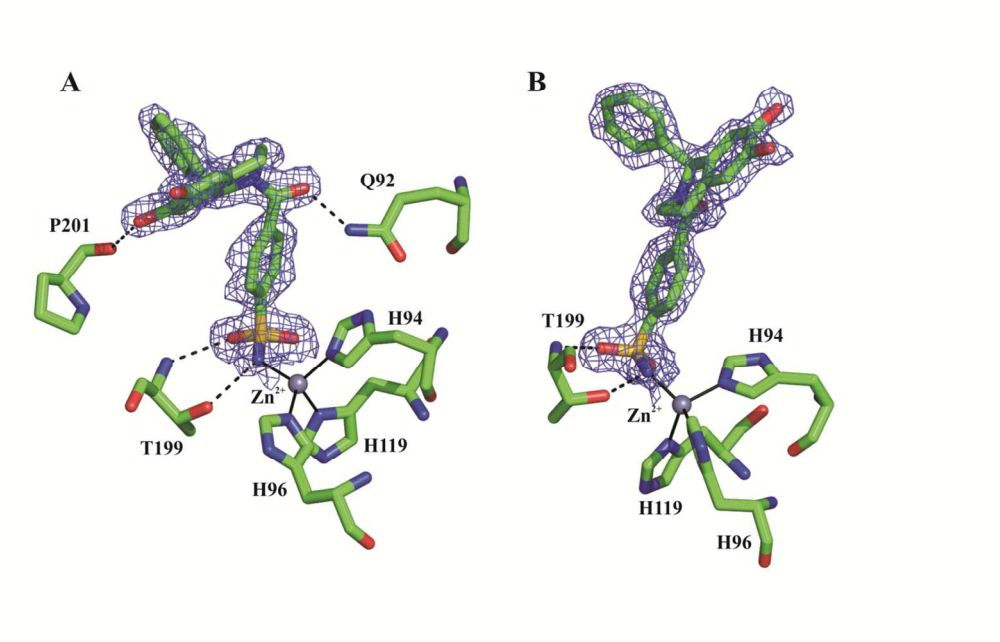
A
P201
Q92
H94
Zn2+
T199
H119
H96
B
T199
H94
Zn2+
H119
H96

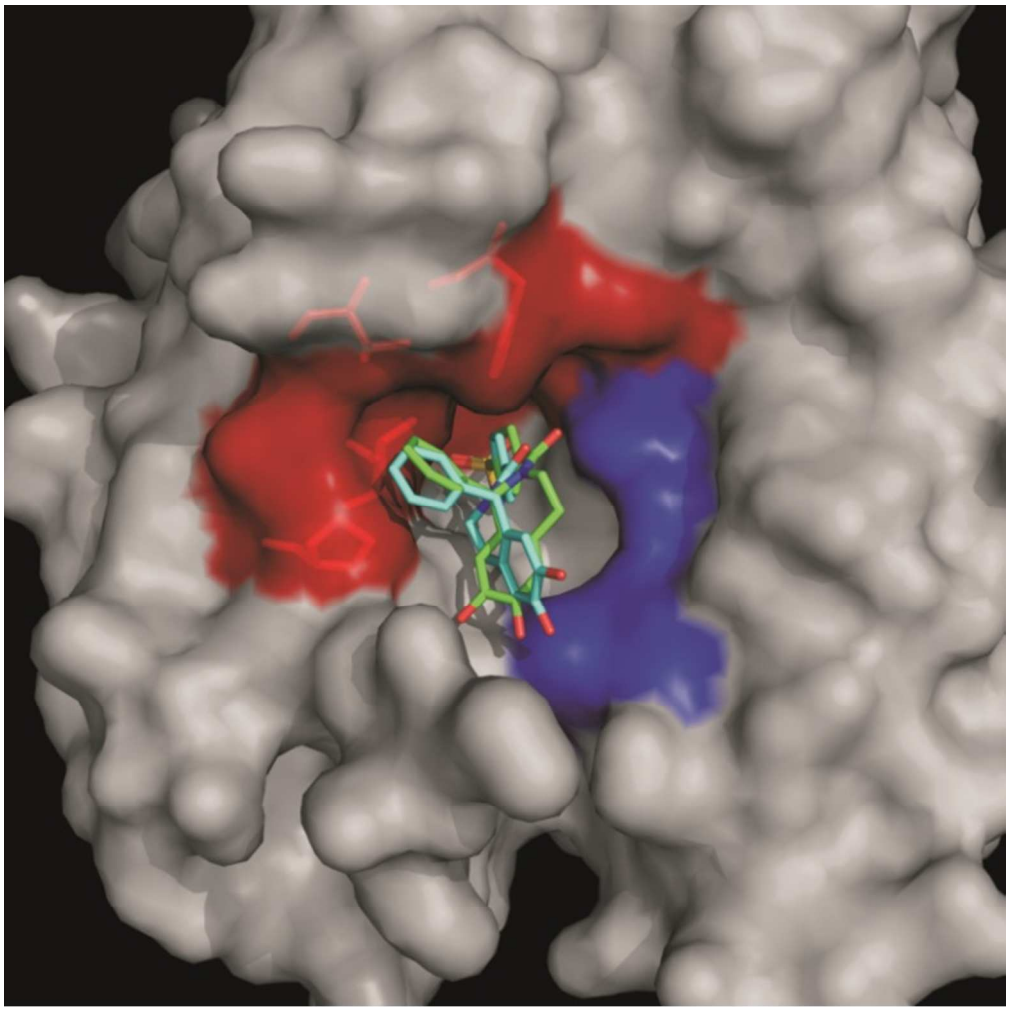

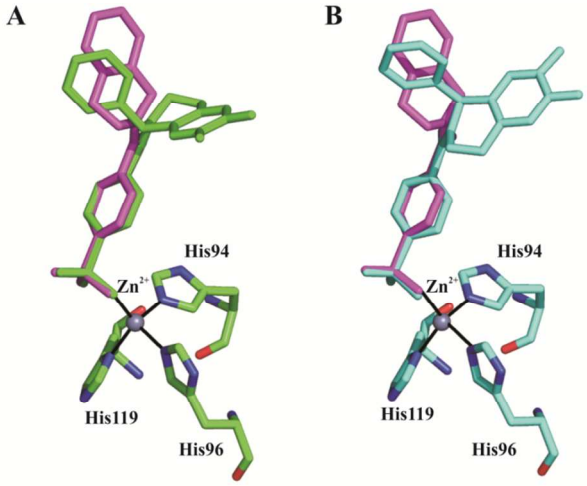
A
His94
Zn2+
His119
His96
B
His94
Zn2+
His119
His96

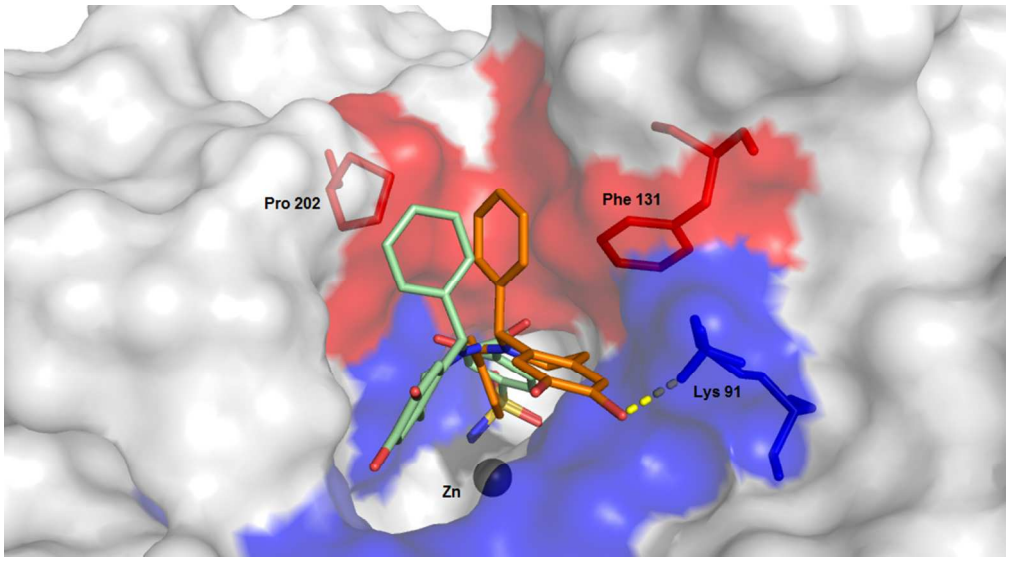
Pro 202
Phe 131
Lys 91
Zn

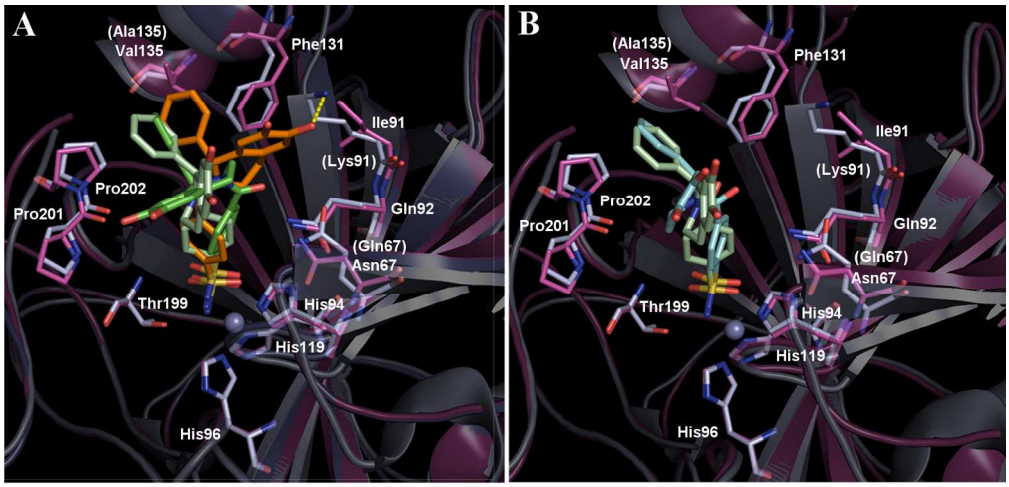
A
(Ala135)
Val135
Phe131
Ile91
(Lys91)
Pro202
Pro201
Gln92
(Gln67)
Asn67
Thr199
His94
His119
His96
B
(Ala135)
Val135
Phe131
Ile91
(Lys91)
Pro202
Pro201
Gln92
(Gln67)
Asn67
Thr199
His94
His119
His96